Title

Pre- and post-contrast three-dimensional double inversion-recovery MRI in human glioblastoma

Journal

Journal of Neuro-Oncology, 112(2)

ISSN

0167-594X

Authors

Harris, Robert J
Cloughesy, Timothy F
Pope, Whitney B
et al.

Publication Date

2013-04-01

DOI

10.1007/s11060-013-1057-y

Peer reviewed

Published in final edited form as:
J Neurooncol. 2013 April ; 112(2): 257–266. doi:10.1007/s11060-013-1057-y.

Pre- and post-contrast three-dimensional double inversion-recovery MRI in human glioblastoma

Robert J. Harris,
Department of Radiological Sciences, David Geffen School of Medicine, University of California Los Angeles, 924 Westwood Blvd., Suite 615, Los Angeles, CA 90024, USA; Department of Biomedical Physics, David Geffen School of Medicine, University of California Los Angeles, Los Angeles, CA, USA

Timothy F. Cloughesy,
Department of Neurology, David Geffen & School of Medicine, University of California Los Angeles, Los Angeles, CA, USA

Whitney B. Pope,
Department of Radiological Sciences, David Geffen School of Medicine, University of California Los Angeles, 924 Westwood Blvd., Suite 615, Los Angeles, CA 90024, USA

Sergio Godinez,
Department of Radiological Sciences, David Geffen School of Medicine, University of California Los Angeles, 924 Westwood Blvd., Suite 615, Los Angeles, CA 90024, USA

Yutaka Natsuaki,
Siemens Healthcare, Magnetic Resonance Research & Development West, Los Angeles, CA, USA

Phioanh L. Nghiemphu,
Department of Neurology, David Geffen & School of Medicine, University of California Los Angeles, Los Angeles, CA, USA

Heiko Meyer,
Siemens Healthcare, Erlangen, Germany

Dominik Paul,
Siemens Healthcare, Erlangen, Germany

Yalda Behbahanian,
Department of Radiological Sciences, David Geffen School of Medicine, University of California Los Angeles, 924 Westwood Blvd., Suite 615, Los Angeles, CA 90024, USA

Albert Lai, and
Department of Neurology, David Geffen & School of Medicine, University of California Los Angeles, Los Angeles, CA, USA

Benjamin M. Ellingson
Department of Radiological Sciences, David Geffen School of Medicine, University of California Los Angeles, 924 Westwood Blvd., Suite 615, Los Angeles, CA 90024, USA; Department of Biomedical Physics, David Geffen School of Medicine, University of California Los Angeles, Los

Correspondence to: Benjamin M. Ellingson.
B. M. Ellingson (✉) bellingson@mednet.ucla.edu.

Angeles, CA, USA; Department of Bioengineering, David Geffen School of Medicine, University of California Los Angeles, Los Angeles, CA, USA

Abstract

Fluid attenuated inversion recovery (FLAIR) MRI sequences have become an indispensible tool for defining the malignant boundary in patients with brain tumors by nulling the signal contribution from cerebro-spinal fluid allowing both regions of edema and regions of non-enhancing, infiltrating tumor to become hyperintense on resulting images. In the current study we examined the utility of a three-dimensional double inversion recovery (DIR) sequence that additionally nulls the MR signal associated with white matter, implemented either pre-contrast or post-contrast, in order to determine whether this sequence allows for better differentiation between tumor and normal brain tissue. T1- and T2-weighted, FLAIR, dynamic susceptibility contrast (DSC)-MRI estimates of cerebral blood volume (rCBV), contrast-enhanced T1-weighted images (T1+C), and DIR data (pre- or post-contrast) were acquired in 22 patients with glioblastoma. Contrast-to-noise (CNR) and tumor volumes were compared between DIR and FLAIR sequences. Line profiles across regions of tumor were generated to evaluate similarities between image contrasts. Additionally, voxel-wise associations between DIR and other sequences were examined. Results suggested post-contrast DIR images were hyperintense (bright) in regions spatially similar those having FLAIR hyperintensity and hypointense (dark) in regions with contrast-enhancement or elevated rCBV due to the high sensitivity of 3D turbo spin echo sequences to susceptibility differences between different tissues. DIR tumor volumes were statistically smaller than tumor volumes as defined by FLAIR (Paired t test, $P = 0.0084$), averaging a difference of approximately 14 mL or 24 %. DIR images had approximately 1.5× higher lesion CNR compared with FLAIR images (Paired t test, $P = 0.0048$). Line profiles across tumor regions and scatter plots of voxel-wise coherence between different contrasts confirmed a positive correlation between DIR and FLAIR signal intensity and a negative correlation between DIR and both post-contrast T1-weighted image signal intensity and rCBV. Additional discrepancies between FLAIR and DIR abnormal regions were also observed, together suggesting DIR may provide additional information beyond that of FLAIR.

Keywords

Double inversion-recovery; DIR; MRI; Glioblastoma; Multiparametric MRI

Introduction

Glioblastoma is a primary central nervous system tumor with a very poor prognosis [1]. Standard anatomical magnetic resonance imaging (MRI) techniques are currently the gold standard for determining treatment response and for monitoring tumor growth and infiltration in glioblastoma. In particular, the use of pre- and post-contrast T1-weighted and T2-weighted images are often used to discern regions of abnormal vascularity, necrosis, edema, and infiltrating tumor, as these are important biological features that provide insight into the aggressiveness of the tumor [2–4]. The use of T2-weighted fluid-attenuated inversion recovery (FLAIR) sequences have become an indispensible tool for defining the malignant boundaries [5–7], as this sequence nulls cerebro-spinal fluid (CSF) allowing both edema and infiltrating tumor to be well demarcated and hyperintense on the resulting images.

Despite the exquisite sensitivity of the FLAIR sequence to these important biological features, the boundaries between edematous tissue and normal white matter can be difficult to delineate, resulting in a degree of uncertainty when defining the malignant boundary. In

order to address these challenges, we tested a three-dimensional double inversion recovery (DIR) sequence that nulls both the signal from CSF as well as the signal from normal white matter. Since similar sequences have been used to isolate subtle white matter lesions in patients with multiple sclerosis (MS) [8], we hypothesized this sequence would allow for superior delineation of the tumor regions from regions of normal white matter. Further, since steady-state T2-weighted sequences are highly sensitive to changes in magnetic susceptibility, we hypothesized that post-contrast DIR images may provide signal attenuation in regions of increased contrast enhancement or blood volume. In the current study, we explored the potential utility of pre- and post-contrast DIR images in patients with glioblastoma by comparing them to conventional T1- and T2-weighted, FLAIR, and dynamic susceptibility contrast (DSC)-MRI imaging sequences.

Methods

Image data was collected from 22 patients with recurrent glioblastoma who had provided consent to have their image data collected and stored in our institution's neuro-oncology database. All image data was acquired on a 3.0T MR system (Siemens MAGNETOM Trio, Siemens Healthcare, Erlangen, Germany). Standard anatomical sequences included T1-weighted turbo spin echo (TE/TR = 2.5/360 ms, slice thickness = 3 mm with no interslice gap, NEX = 2, matrix size = 320 × 224, and FOV = 24 cm), T2 weighted turbo spin echo (TE/TR = 94/3,500 ms, slice thickness = 3 mm with no interslice gap, NEX = 2, matrix size = 384 × 320, and FOV = 24 cm), and FLAIR images (TI = 2,500 ms, TE/TR = 90/8,500 ms, slice thickness = 3 mm with no interslice gap, NEX = 1, matrix size = 320 × 224, and FOV = 24 cm). Dynamic susceptibility contrast (DSC) images (TE = 25 ms, TR = 1,250 ms, flip angle = 35 degrees, slice thickness = 3 mm with no interslice gap, matrix size 128 × 128, GRAPPA = 2; 6/8 partial Fourier encoding) were acquired during injection of a gadopentetate dimeglumine (Magnevist; Berlex, Wayne, NJ; 0.075 mmol/kg) bolus, after injection of a ¼ dose preload (0.025 mmol/kg body weight). Intensity standardized rCBV maps were calculated by previously published methods [9] and commercially available software (IB Neuro v2.0; Imaging Biometrics, Elm Grove, Wisconsin). Additionally, contrast-enhanced T1 weighted images (T1 + C; TE/TR = 2.5/360 ms, slice thickness = 3 mm with no interslice gap, NEX = 2, matrix size = 320 × 224, and FOV = 24 cm) were acquired after DSC data.

The non-selective DIR prepared turbo spin echo (TSE) sequence with variable flip angle evolutions (Sampling Perfection with Application optimized Contrasts using different flip angle Evolutions (SPACE), IPR#697; Neuro-SPACE) was utilized for both pre and post-contrast comparisons. The sequence features 2 non-selective IR pulses, with the 2nd IR pulse having a fixed inversion time of TI_2 = 450 ms, to suppress normal-appearing white matter (NAWM). The first TI (TI_1) and TR were adjusted for optimal CSF suppression. 3D SPACE signal readout follows the DIR preparation. An inherent advantage of the 3D SPACE readout compared to the conventional 2D TSE involves the pre-calculation of signal evolution in order to employ variable flip angles to maintain magnetization for longer echo train lengths in order generate desired T1 or T2 contrasts. This also allows for the acquisition of an isotropic 3D volume with high resolution in a clinically feasible scan time. The following DIR sequence parameters were used for both pre- and post-contrast acquisitions: TE/TR = 324/7,400 ms, slice thickness = 1.3 mm, matrix size = 192 × 192, FOV = 25 cm, TI_1 = 3,000 ms, and TI_2 = 450 ms.

All images from all patients were registered to the respective DIR images using a mutual information algorithm and a 12-degree of freedom transformation using FSL (FMRIB, Oxford, UK; http://www.fmrib.ox.ac.uk/fsl/) to ensure correct voxel-wise comparisons between the images. Manual adjustment, if necessary, was performed using the *tkregister2*

routine available from Freesurfer (surfer.nmr.mgh.harvard.edu; Massachusetts General Hospital—Harvard Medical School, Boston, MA). Tumor regions of interest (ROIs) were defined on both pre- and post-contrast DIR and FLAIR images using a semi-automated thresholding technique employed previously [10]. It is important to note that the entire abnormal area on post-contrast DIR images were included in the calculation of hyperintense volumes (i.e. regions of signal dropout on DIR corresponding to contrast-enhancement were also included). The mean differences in tumor volume between DIR and FLAIR hyperintense regions were compared using a paired *t* test. Contrast-to-noise ratio (CNR), defined as the difference in mean signal intensity between the tumor and normal appearing white matter divided by the standard deviation of background noise ($|\mu_{TUMOR}-\mu_{WM}|/\sigma_{NOISE}$), was calculated for both DIR and FLAIR images then compared using a paired *t* test. Line profiles were created across tumor regions for qualitatively comparing the different image sequences using custom MATLAB scripts (MATLAB; Mathworks, Inc., Natick, MA). Additionally, four circular ROIs were placed in separate regions of the brain in each patient such that approximately half the ROI contained T2 hyperintense tumor and half the area contained normal appearing tissue. These ROIs were then used to generate scatter plots examining the voxel-wise correlations between the different imaging contrasts.

The Institutional Review Board at our institution approved all protocols.

Results

In general, DIR images provided a high level of contrast between suspected tumor regions and background white matter tissue due to suppression of both white matter and CSF signal intensity (Fig. 1). Regions of suspected tumor and the cortical ribbon both appear hyperintense on DIR; however, the signal intensity within suspected tumor regions were consistently higher in signal amplitude than normal cortex. This difference in signal intensity, along with the hypointensity of white matter, allowed for clear identification of edema from non-enhancing tumor in regions near the cortex, since edema tends to preserve the cortical ribbon (Fig. 1e) and non-enhancing tumor degrades the cortical architecture [11–13]. In cases where DIR acquisition occurred after contrast agent injection (Fig. 1f–j), images appeared to show clear signal attenuation in regions with contrast enhancement and/or elevated rCBV.

DIR scans were obtained in a single patient before and after administration of bevacizumab, an anti-angiogenic agent known to reduce the about of vascular permeability and edema (Fig. 2). A single treatment with bevacizumab resulted in a decrease in contrast enhancement on post-contrast T1-weighted images, a decrease in rCBV, and a decrease in T2 hyperintensity on T2-weighted, FLAIR, and DIR images. Interesting, the volume of contrast enhancement decreased by 71 % and the volume of T2 hyperintensity decreased by 46 %; however, the volume of DIR hyperintensity decreased by more than 62 %, suggesting T2 and FLAIR hyperintense regions may be sensitive to slightly different tissue types compared with DIR hyperintense regions.

When visually examining post-contrast DIR and FLAIR images in patients with glioblastoma, around 18 % (4 in 22) patients showed conspicuous differences between the two image contrasts (Fig. 3). For example, Fig. 3 illustrates example patients with identifiable FLAIR hyperintensity (“a” through “d”), but no obvious abnormal signal intensity on post-contrast DIR. Consistent with this observed difference with T2 and FLAIR hyperintense volumes, the volume of FLAIR-defined tumor regions was found to be significantly larger than that of DIR-defined tumor regions (Fig. 4a; Paired *t* test, $P = 0.0084$), with an average difference in volume of approximately 14 mL (Fig. 4b). The percentage difference between these regions with respect to FLAIR volume was

significantly different from zero (Fig 4c; *t* test, $P = 0.0068$), with FLAIR-defined hyperintense lesions having approximately 24 % higher volume compared with DIR hyperintense lesion volume. As expected, the mean CNR between the tumor regions and NAWM were higher in the DIR images compared with FLAIR, averaging 122.8 ± 13.2 S.E.M. for DIR images and 77.8 ± 12.3 S.E.M. for the FLAIR images (Fig. 4d; Paired *t* test, $P = 0.0048$). Only four patients had FLAIR images with higher CNR compared with DIR images, for which all had a relatively high variability of the tumor signal intensity in the DIR images compared with FLAIR regions leading to lower calculated CNR.

We hypothesized that a high positive spatial correlation exists between FLAIR and DIR images, since these regions both are theoretically sensitive to T2 hyperintensity and both have CSF signal nulling. Additionally, we hypothesized that a negative spatial correlation will exist between post-contrast DIR images and regions with high rCBV and contrast-enhancing regions on post-contrast T1-weighted images due to the sensitivity of the SPACE base sequence to field inhomogeneities caused by the presence of gadolinium. To test these hypotheses we created line profiles starting in regions of normal tissue and extending into tumorous regions (Fig. 5a–d for 4 select patients). Results revealed a strong positive qualitative relationship between FLAIR and DIR image intensity (Fig. 5e–h), as well as a strong negative correlation between rCBV and T1+C image intensity compared with DIR image intensity (Fig. 5i–l).

The nature of this relationship is further appreciated by examining the voxel-wise correlation between post-contrast DIR, FLAIR, T1+C, and rCBV images (Fig. 6). When mapped to their original locations, low signal intensity regions on post-contrast DIR and mid-range signal intensity on FLAIR were localized to regions of white matter, mid-range signal intensity regions on both DIR and FLAIR corresponded to regions of gray matter, and hyperintense regions on both DIR and FLAIR corresponded to regions of abnormal T2/FLAIR signal intensity indicative of either tumor or edema (Fig. 6a). This positive voxel-wise relationship between post-contrast DIR and FLAIR signal intensity was statistically significant and similar for all patients examined (Pearson's correlation coefficient, $R^2 > 0.6$, $P < 0.001$). When comparing the voxel-wise correlation between post-contrast DIR and post-contrast T1-weighted images, voxels with low signal intensity on both post-contrast DIR and post-contrast T1-weighted images were localized to white matter, regions with low post-contrast DIR signal intensity but high signal intensity on post-contrast T1-weighted images corresponded to regions of contrast-enhancing tumor, mid-range post-contrast DIR signal intensities and mid-range post-contrast T1-weighted signal intensities corresponded to regions of gray matter, while voxels exhibiting elevated post-contrast DIR signal intensity and hypointensity on post-contrast T1-weighted images were localized to regions having abnormal T2/FLAIR signal intensity reflecting either non-enhancing tumor or edema (Fig. 6h). The negative correlation observed between post-contrast DIR and post-contrast T1-weighted images was also statistically significant and similar for all patients examined (Pearson's correlation coefficient, $R^2 > 0.6$, $P < 0.001$). Voxel-wise comparison of post-contrast DIR images with rCBV maps created from DSC-MRI also illustrated a negative correlation between signal intensities, albeit slightly more complex than the relationship between post-contrast DIR and post-contrast T1-weighted images. Specifically, voxels exhibiting low signal intensity on post-contrast DIR images and low rCBV were spatially localized to regions of white matter, voxels with slightly higher signal intensity on DIR and slightly higher rCBV reflected regions of gray matter, voxels with low signal intensity on DIR and high rCBV reflected aggressive regions of tumor within contrast-enhancing regions, and voxels with high signal intensity on post-contrast DIR images but low rCBV were localized to regions of abnormal T2/FLAIR signal intensity (Fig. 6i). Similar to the comparison between post-contrast DIR and post-contrast T1-weighted images, there was also a significant negative correlation between post-contrast DIR and rCBV that was similar

between all patients (Pearson's correlation coefficient, $R^2 > 0.6$, $P < 0.001$). Together, these results support the hypothesis that hyperintense regions on post-contrast DIR images generally reflect the T2/FLAIR hyperintense regions, whereas regions of decreased signal intensity on post-contrast DIR images within these hyperintense lesions reflect regions of contrast-enhancement on post-contrast T1-weighted images and regions of elevated tumor blood volume on DSC-MRI derived rCBV maps.

Discussion

T2-weighted FLAIR remains the most sensitive MR pulse sequence for identifying the malignant boundary in human glioblastoma [5–7]; however, FLAIR sequences are relatively non-specific, showing sensitivity to both vasogenic edema and non-enhancing/infiltrating tumor. Therefore, there is a need for new MR sequences that add value to the current FLAIR sequence. In the current study we explored the ability for a DIR sequence to improve upon FLAIR with additional nulling of NAWM. We hypothesized that the DIR sequence may offer additional insight into the boundary of T2 hyperintense lesions that may be difficult to delineate from either the cortex or white matter. Additionally, we hypothesized that post-contrast DIR images would not only show similar hyperintense regions to FLAIR, but also provide localization of regions with contrast-enhancement or elevated tumor blood volume since signal dropout occurs in regions of susceptibility differences due to the nature of the 3D TSE sequence. Consistent with these hypotheses, results from the current study suggest that hyperintense lesions on 3D DIR images correlate spatially with hyperintense lesions on FLAIR images, although FLAIR tended to overestimate the suspected lesion volume and had lower CNR compared with DIR. Additionally, results demonstrated a strong negative correlation between post-contrast DIR image intensity and both post-contrast T1-weighted signal intensity as well as rCBV. Together, these results imply that post-contrast DIR can capture many important malignant features from other pulse sequences and may indeed add some benefit to traditional FLAIR images.

To the best of our knowledge, this is the first study to examine the potential advantages of DIR imaging in human gliomas; however, the DIR sequence has been implemented extensively and quite successfully for the identification and characterization of subcortical MS lesions. Overwhelming evidence suggests the DIR sequence provides higher sensitivity for the identification of MS lesions compared to either T2 or FLAIR sequences [8, 14–19], leading to the consensus recommendation for use of DIR in scoring of MS lesions [20]. DIR has also been shown to be useful for lesion detection and volume quantification in other types of brain lesions, including identification of epileptic foci [21, 22], hippocampal sclerosis lesions [23, 24], and subcortical band heterotopia [25]. Consistent with observations from studies involving other pathologies, results from the current study suggest the DIR sequence may provide added benefits for delineating the T2 hyperintense lesion from surrounding tissues. Further research is necessary to determine whether DIR is equally superior to FLAIR in terms of the sensitivity to new lesion detection, or whether DIR can better determine the extent of tumor infiltration into normal white matter.

There are a few potential study limitations that merit attention. First, the current study involved a series of glioblastoma patients at various stages of their disease and on various treatment paradigms. Some patients were currently being treated with the standard of care (i.e. temozolomide and radiotherapy) [26], whereas others (including the patient in Fig. 2) were treated with bevacizumab or other anti-angiogenic agents. Although the purpose of the current study was purely investigative and the objective was to compare DIR with FLAIR and other sequences, this heterogeneity in the patient population was a potential limitation since the size of T2 hyperintense lesions were likely to be related to particular stage of the disease. Also, we chose to collect pre- and post-contrast DIR images in different

glioblastoma patients in order to save time during their routine clinical MR examination. A more thorough comparison between pre- and post-contrast DIR images could have been performed if pre- and post-contrast DIR images were collected in the same patients. Lastly, the current study did not involve any test–retest reliability testing nor did it involve examining serial DIR imaging in the same patient over time to examine changes in lesion volume. It is possible the DIR systematically underestimates lesion volumes in the same patient compared with FLAIR for all time points; however, it is also possible that the observed differences between DIR and FLAIR may differ by patient or by follow-up time point. Future studies will focus on addressing these potential limitations.

We hypothesize that the DIR sequence used in the current study may be improved for better delineation of non-enhancing tumor. Based on previous studies, the DIR sequence is known to provide exceptional sensitivity for lesion detection when slightly prolonged T2 is anticipated compared with the nulled tissues [27], suggesting using inversion times specific for nulling CSF and NAWM may result in DIR contrasts without an advantage over FLAIR sequences. Alternatively, the inversion pulse used to null NAWM could be adjusted to null signal from vasogenic edema exclusively, since infiltrating/non-enhancing tumr and vasogenic edema have very subtle differences in T2 characteristics, which may lead to better contrast between these tissue types. Additionally, the use of a phase-sensitive inversion recovery (PSIR) sequence, where values can be positive and negative based on the initial magnetization after inversion preparation, may provide additional benefits to DIR in terms of lesion detection and characterization, as has been demonstrated for MS lesions [28, 29].

Conclusion

Results from the current study suggest pre- or post-contrast DIR may provide information beyond that of T2-weighted FLAIR images. Specifically, FLAIR images tended to overestimate lesion volume and have lower lesion CNR compared to DIR. Also, post-contrast DIR signal intensity is positively correlated with FLAIR images and negatively correlated with post-contrast T1-weighted signal intensity and rCBV.

Acknowledgments

Funding UCLA Institute for Molecular Medicine Seed Grant (BME); UCLA Radiology Exploratory Research Grant (BME); University of California Cancer Research Coordinating Committee Grant (BME); ACRIN Young Investigator Initiative Grant (BME); Art of the Brain (TFC); Ziering Family Foundation in memory of Sigi Ziering (TFC); Singleton Family Foundation (TFC); Clarence Klein Fund for Neuro-Oncology (TFC).

References

1. Lima FR, Kahn SA, Soletti RC, Biasoli D, Alves T, da Fonseca AC, Garcia C, Romao L, Brito J, Holanda-Afonso R, Faria J, Borges H, Moura-Neto V. Glioblastoma: therapeutic challenges, what lies ahead. Biochim Biophys Acta. 1826:338–349. 2012.
2. Mouthuy N, Cosnard G, Abarca-Quinones J, Michoux N. Multiparametric magnetic resonance imaging to differentiate high-grade gliomas and brain metastases. J Neuroradiol. 2011; 39(5):301–307. [PubMed: 22197404]
3. Iliadis G, Kotoula V, Chatzisotiriou A, Televantou D, Eleftheraki AG, Lambaki S, Misailidou D, Selviaridis P, Fountzilas G. Volumetric and MGMT parameters in glioblastoma patients: survival analysis. BMC Cancer. 2012; 12:3. [PubMed: 22214427]
4. Farace P, Giri MG, Meliado G, Amelio D, Widesott L, Ricciardi GK, Dall'Oglio S, Rizzotti A, Sbarbati A, Beltramello A, Maluta S, Amichetti M. Clinical target volume delineation in glioblastomas: pre-operative versus post-operative/pre-radiotherapy MRI. Br J Radiol. 2011; 84:271–278. [PubMed: 21045069]

5. Tsuchiya K, Mizutani Y, Hachiya J. Preliminary evaluation of fluid-attenuated inversion-recovery MR in the diagnosis of intracranial tumors. AJNR Am J Neuroradiol. 1996; 17:1081–1086. [PubMed: 8791919]
6. Husstedt HW, Sickert M, Kostler H, Haubitz B, Becker H. Diagnostic value of the fast-FLAIR sequence in MR imaging of intracranial tumors. Eur Radiol. 2000; 10:745–752. [PubMed: 10823626]
7. Essig M, Hawighorst H, Schoenberg SO, Engenhart-Cabillic R, Fuss M, Debus J, Zuna I, Knopp MV, van Kaick G. Fast fluid-attenuated inversion-recovery (FLAIR) MRI in the assessment of intraaxial brain tumors. J Magn Reson Imaging. 1998; 8:789–798. [PubMed: 9702879]
8. Geurts JJ, Pouwels PJ, Uitdehaag BM, Polman CH, Barkhof F, Castelijns JA. Intracortical lesions in multiple sclerosis: improved detection with 3D double inversion-recovery MR imaging. Radiology. 2005; 236:254–260. [PubMed: 15987979]
9. Bedekar D, Jensen T, Schmainda KM. Standardization of relative cerebral blood volume (rCBV) image maps for ease of both inter- and intrapatient comparisons. Magn Reson Med. 2010; 64:907–913. [PubMed: 20806381]
10. Ellingson BM, Cloughesy TF, Lai A, Nghiemphu PL, Mischel PS, Pope WB. Quantitative volumetric analysis of conventional MRI response in recurrent glioblastoma treated with bevacizumab. Neuro Oncol. 2011; 13:401–409. [PubMed: 21324937]
11. Pope WB, Sayre J, Perlina A, Villablanca JP, Mischel PS, Cloughesy TF. MR imaging correlates of survival in patients with high-grade gliomas. AJNR Am J Neuroradiol. 2005; 26:2466–2474. [PubMed: 16286386]
12. Pope WB, Chen JH, Dong J, Carlson MR, Perlina A, Cloughesy TF, Liau LM, Mischel PS, Nghiemphu P, Lai A, Nelson SF. Relationship between gene expression and enhancement in glioblastoma multiforme: exploratory DNA microarray analysis. Radiology. 2008; 249:268–277. [PubMed: 18796682]
13. Felsberg GJ, Silver SA, Brown MT, Tien RD. Radiologicpathologic correlation. Gliomatosis cerebri. AJNR Am J Neuroradiol. 1994; 15:1745–1753. [PubMed: 7847223]
14. Seewann A, Kooi EJ, Roosendaal SD, Pouwels PJ, Wattjes MP, van der Valk P, Barkhof F, Polman CH, Geurts JJ. Post-mortem verification of MS cortical lesion detection with 3D DIR. Neurology. 2012; 78:302–308. [PubMed: 22218278]
15. Coebergh JA, Roosendaal SD, Polman CH, Geurts JJ, van Woerkom TC. Acute severe memory impairment as a presenting symptom of multiple sclerosis: a clinical case study with 3D double inversion recovery MR imaging. Mult Scler. 2010; 16:1521–1524. [PubMed: 20846999]
16. Simon B, Schmidt S, Lukas C, Gieseke J, Traber F, Knol DL, Willinek WA, Geurts JJ, Schild HH, Barkhof F, Wattjes MP. Improved in vivo detection of cortical lesions in multiple sclerosis using double inversion recovery MR imaging at 3 Tesla. Eur Radiol. 2010; 20(7):1675–1683. [PubMed: 20094887]
17. Moraal B, Roosendaal SD, Pouwels PJ, Vrenken H, van Schijndel RA, Meier DS, Guttmann CR, Geurts JJ, Barkhof F. Multi-contrast, isotropic, single-slab 3D MR imaging in multiple sclerosis. Eur Radiol. 2008; 18:2311–2320. [PubMed: 18509658]
18. Roosendaal SD, Moraal B, Vrenken H, Castelijns JA, Pouwels PJ, Barkhof F, Geurts JJ. In vivo MR imaging of hippocampal lesions in multiple sclerosis. J Magn Reson Imaging. 2008; 27(4): 726–731. [PubMed: 18302199]
19. Wattjes MP, Lutterbey GG, Gieseke J, Traber F, Klotz L, Schmidt S, Schild HH. Double inversion recovery brain imaging at 3T: diagnostic value in the detection of multiple sclerosis lesions. AJNR Am J Neuroradiol. 2007; 28:54–59. [PubMed: 17213424]
20. Geurts JJ, Roosendaal SD, Calabrese M, Ciccarelli O, Agosta F, Chard DT, Gass A, Huerga E, Moraal B, Pareto D, Rocca MA, Wattjes MP, Yousry TA, Uitdehaag BM, Barkhof F. Consensus recommendations for MS cortical lesion scoring using double inversion recovery MRI. Neurology. 2011; 76:418–424. [PubMed: 21209373]
21. Morimoto E, Kanagaki M, Okada T, Yamamoto A, Mori N, Matsumoto R, Ikeda A, Mikuni N, Kunieda T, Paul D, Miyamoto S, Takahashi R, Togashi K. Anterior temporal lobe white matter abnormal signal (ATLAS) as an indicator of seizure focus laterality in temporal lobe epilepsy:

comparison of double inversion recovery, FLAIR and T2W MR imaging. Eur Radiol. 2012; 23(1): 3–11. [PubMed: 22811046]

22. Rugg-Gunn FJ, Boulby PA, Symms MR, Barker GJ, Duncan JS. Imaging the neocortex in epilepsy with double inversion recovery imaging. Neuroimage. 2006; 31(1):39–50. [PubMed: 16460962]
23. Li Q, Zhang Q, Sun H, Zhang Y, Bai R. Double inversion recovery magnetic resonance imaging at 3 T: diagnostic value in hippocampal sclerosis. J Comput Assist Tomogr. 2011; 35:290–293. [PubMed: 21412105]
24. Zhang Q, Li Q, Zhang J, Zhang Y. Double inversion recovery magnetic resonance imaging (MRI) in the preoperative evaluation of hippocampal sclerosis: correlation with volumetric measurement and proton magnetic resonance spectroscopy (^{1}HMRS). J Comput Assist Tomogr. 2011; 35:406–410. [PubMed: 21586939]
25. Zhang Q, Zhang Y, Zhang J, Li Q. Double inversion recovery magnetic resonance imaging of subcortical band heterotopia: a report of 2 cases. J Comput Assist Tomogr. 2011; 35:31–32. [PubMed: 21245686]
26. Stupp R, Mason WP, van den Bent MJ, Weller M, Fisher B, Taphoorn MJ, Belanger K, Brandes AA, Marosi C, Bogdahn U, Curschmann J, Janzer RC, Ludwin SK, Gorlia T, Allgeier A, Lacombe D, Cairncross JG, Eisenhauer E, Mirimanoff RO. Radiotherapy plus concomitant and adjuvant temozolomide for glioblastoma. N Engl J Med. 2005; 352:987–996. [PubMed: 15758009]
27. Turetschek K, Wunderbaldinger P, Bankier AA, Zontsich T, Graf O, Mallek R, Hittmair K. Double inversion recovery imaging of the brain: initial experience and comparison with fluid attenuated inversion recovery imaging. Magn Reson Imaging. 1998; 16:127–135. [PubMed: 9508269]
28. Sethi V, Yousry TA, Muhlert N, Ron M, Golay X, Wheeler-Kingshott C, Miller DH, Chard DT. Improved detection of cortical MS lesions with phase-sensitive inversion recovery MRI. J Neurol Neurosurg Psychiatry. 2012; 83:877–882. [PubMed: 22807559]
29. Nelson F, Poonawalla AH, Hou P, Huang F, Wolinsky JS, Narayana PA. Improved identification of intracortical lesions in multiple sclerosis with phase-sensitive inversion recovery in combination with fast double inversion recovery MR imaging. AJNR Am J Neuroradiol. 2007; 28:1645–1649. [PubMed: 17885241]

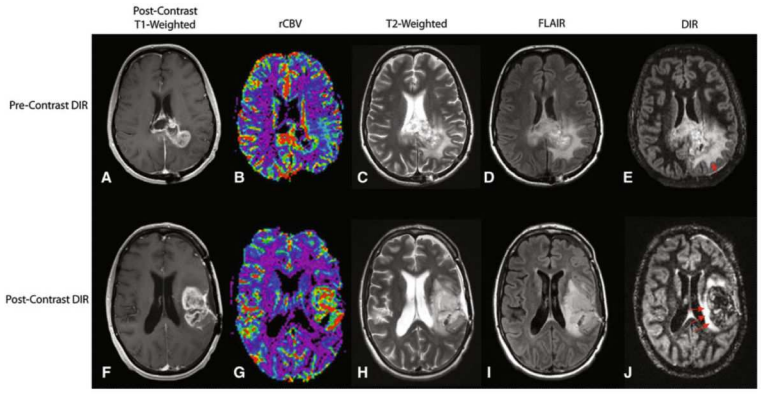

Fig. 1.

Multiparametric and pre- or post-contrast double inversion recovery (DIR) images in human glioblastoma. **a** Post-contrast T1-weighted image, **b** relative cerebral blood volume (rCBV) map, **c** T2-weighted image, **d** FLAIR image, and **e** pre-contrast DIR image in a 48 year old female patient with a glioblastoma. *Arrows* in **e** denote regions of thought to contain primarily vasogenic edema due to preservation of the cortical ribbon. **f** Post-contrast T1-weighted image, **g** rCBV map, **h** T2-weighted image, **i** FLAIR image, and **j** post-contrast DIR image in a 54 year old female patient with glioblastoma. *Arrows* in (**j**) show signal dropout on post-contrast DIR images corresponding to regions of contrast enhancement and elevated rCBV

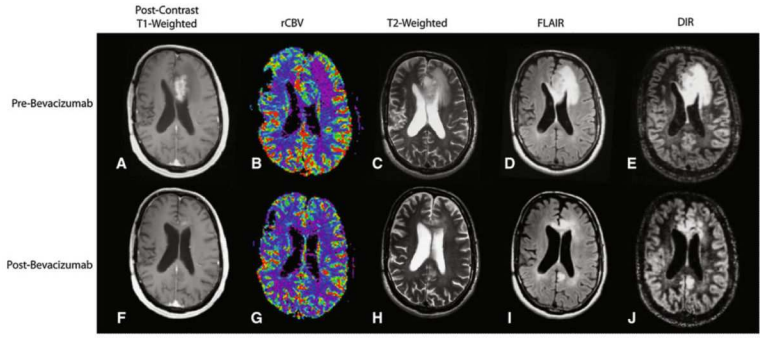

Fig. 2.

DIR images of human glioblastoma before and after administration of the anti-angiogenic agent bevacizumab. **a** Post-contrast T1-weighted images, **b** rCBV maps, **c** T2-weighted images, **d** FLAIR images, and **e** pre-contrast DIR images before administration of bevacizumab in a 57 year old male patient with recurrent glioblastoma. **f** Post-contrast T1-weighted iamges, **g** rCBV maps, **h** T2-weighted images, **i** FLAIR images, and **j** pre-contrast DIR images after administration of bevacizumab, demonstrating significant reduction in contrast enhancement, rCBV, and hyperintense lesion volume on T2-weighted, FLAIR, and DIR images

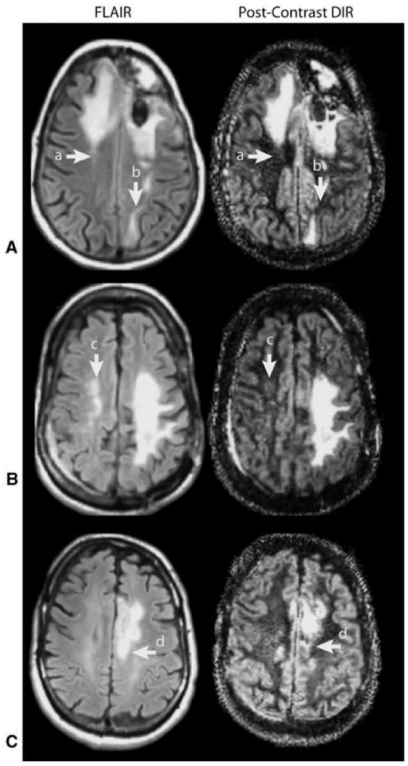

Fig. 3.

Conspicuous signal abnormalities that differ between FLAIR and DIR images. **a** Abnormal FLAIR signal intensity within the right frontal lobe extending posterior (“a”) that is not observed on DIR images. Similarly, a FLAIR hyperintense lesion in the left parietal lobe is observed extending inferior into white matter regions (“b”), but this was not observed on DIR images. **b** Abnormal FLAIR signal intensity in the right hemisphere (“c”), contralateral from the original tumor location, is not clearly apparent on DIR images. **c** Posterior aspect of a lesion in the left frontal lobe observed on FLAIR (“d”) did not demonstrate substantial hyperintensity on DIR imagesb

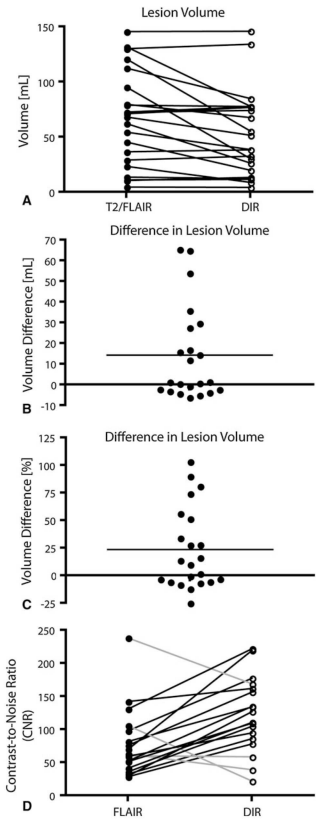

Fig. 4.

Lesion volume and contrast-to-noise ratio (CNR) comparisons between FLAIR and DIR. **a** Lesion volume comparisons between FLAIR and DIR images suggests FLAIR may overestimate lesion volume compared to DIR images (Paired *t* test, $P = 0.0084$). **b** Volume difference between FLAIR and DIR demonstrating FLAIR lesion volumes having an average difference of 14 mL compared with DIR lesions. **c** Percent volume differences between FLAIR and DIR showing FLAIR lesion volumes having an average of 24 % higher volumes compared with DIR lesion volume estimates. **d** Lesion CNR in FLAIR and DIR showing a significantly higher CNR in DIR compared with FLAIR images (Paired *t* test, $P = 0.0048$). *Gray lines* show four cases where FLAIR had higher CNR compared to DIR

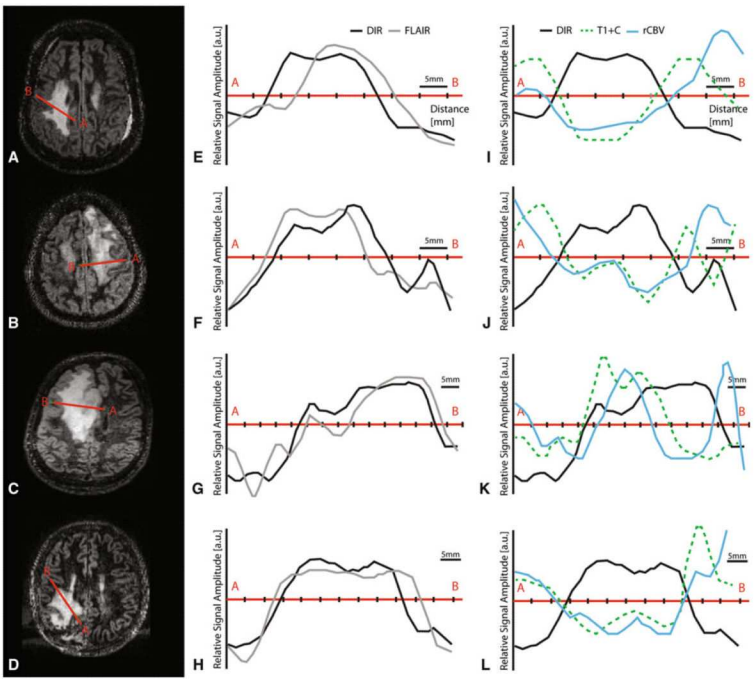

Fig. 5.

Line profiles through tumor regions in four patients with glioblastoma, demonstrating spatial correlation between post-contrast DIR images and multiparametric MRI. **a–d**) Post-contrast DIR images showing the location of the corresponding line profiles (*red lines* with "*A*" and "*B*"). **e–h** Line profiles for DIR (*black*) and FLAIR (*gray*) showing a strong spatial correlation between these two image contrasts. **i–l** Line profiles for DIR (*black*), post-contrast T1-weighted images (T1+C; *dashed green*), and rCBV (*blue line*) demonstrating a negative spatial correlation between these image contrasts within tumor regions

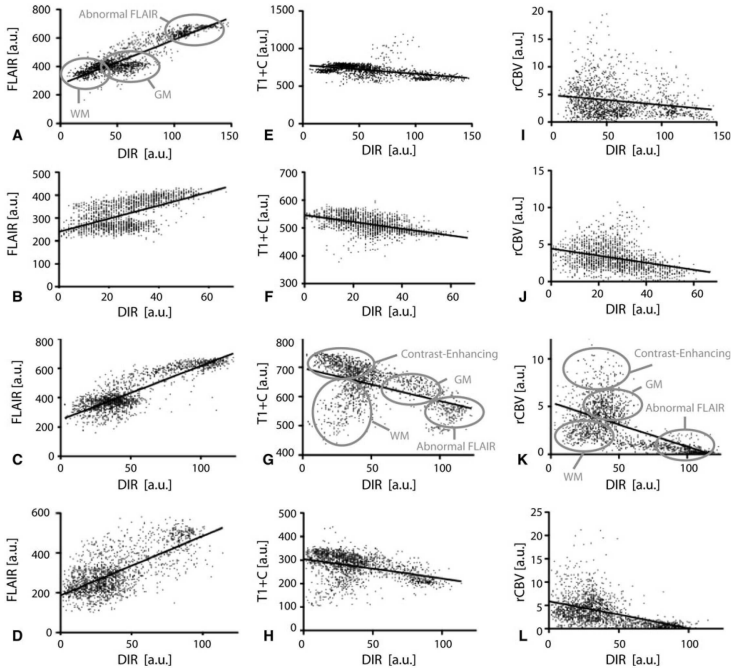

Fig. 6.

Voxel-wise coherence between DIR and multiparametric MR images. **a–d** Voxel-wise associations between FLAIR and DIR signal intensities show a positive linear correlation (Pearson's correlation coefficient, $R^2 > 0.6$, $P < 0.001$ for all patients examined). Note that mid-range signal intensity on FLAIR and low signal intensity on DIR corresponded primarily to white matter (WM), mid-range signal intensity on both FLAIR and DIR corresponded to gray matter (GM), while high signal intensity on both FLAIR and DIR corresponded to regions with abnormal T2/FLAIR signal intensity. **e–f** Voxel-wise associations between post-contrast T1-weighted (T1+C) and DIR signal intensities show a negative linear correlation (Pearson's correlation coefficient, $R^2 > 0.6$, $P < 0.001$ for all patients examined). Note that voxels with mid-range signal intensity on T1+C and low signal intensity on DIR corresponded to WM, voxels with mid-range signal intensity on both T1+C and DIR corresponded to GM, voxels with low-signal intensity on T1+C and high signal intensity on DIR corresponded to regions with abnormal T2/FLAIR signal intensity, and voxels with high signal intensity on T1+C and low signal intensity on DIR corresponded to regions with contrast-enhancement. **i–l** Voxel-wise associations between rCBV and DIR signal intensities showing a negative linear correlation (Pearson's correlation coefficient, $R^2 > 0.6$, $P < 0.001$ for all patients examined). Note that voxels with high rCBV and low signal intensity on DIR corresponded to regions of contrast-enhancement and hypervascular tumor, voxels with low rCBV and low signal intensity on DIR corresponded to WM, voxels with mid-range values of both rCBV and DIR signal intensity corresponded to GM, and voxels with low rCBV and high DIR signal intensity corresponded to regions with abnormal T2/FLAIR signal intensities